

High System Performance with Plasmonic Waveguides and Functional Devices

Wing-Ying Kwong

Photonics offers a solution to data communication between logic devices in computing systems; however, the integration of photonic components into electronic chips is rather limited due to their size incompatibility. Dimensions of photonic components are therefore being forced to be scaled down dramatically to achieve a much higher system performance. To integrate these nano-photonic components, surface plasmon-polaritons and/or energy transfer mechanisms are used to form plasmonic chips. In this paper, the operating principle of plasmonic waveguide devices is reviewed within the mid-infrared spectral region at the 2 μm to 5 μm range, including lossless signal propagation by introducing gain. Experimental results demonstrate that these plasmonic devices, of sizes approximately half of the operating free-space wavelengths, require less gain to achieve lossless propagation. Through optimization of device performance by means of methods such as the use of new plasmonic waveguide materials that exhibit a much lower minimal loss value, these plasmonic devices can significantly impact electronic systems used in data communications, signal processing, and sensors industries.

Keywords: Surface plasmon, plasmonic, nano-photonic, metal, waveguide, functional device, infrared, sub-wavelength.

I. Introduction

The application of photonics in computing and information processing has been discussed over the past several decades. Impacted current computing systems consist of intra- and inter-chip interconnections that rely upon the flow of photons, thereby solving the communication problem between logic devices. In addition, photonics can also reduce the total operating energy of a digital logic system and the physical size of a chip. The influence of nano-technology in integrated optics—the third generation of photonic device technology—not only solves the ever-increasing data-transfer capacity problem, speeding-up electronic computer processing, but also allows computer chips to be miniaturized, enabling these data to route in sub-wavelength dimensions. Consequently, the cost of expensive optical components can be reduced and a higher system performance can be obtained.

Recent investigations into electromagnetic properties of nano-structured waveguide materials have renewed interest in surface plasmons (quanta of collective excitations), with their applications being led to a new area of plasmonics, namely, surface-plasmon-based photonics. In a plasmonic integrated circuit, optical signals and electric current are carried concurrently through waveguide nano-structures. That is, optical signals propagate along the surface of conducting metals or active control-electrodes. This light-metal interaction gives rise to surface plasmon-polariton (SPP) electromagnetic modes that have a greater momentum than light at any particular optical frequency and are strongly confined to and guided by the planar metallic surface, where mobile electron-charges reside. These modes can be controlled by guided waves from surrounding dielectric media and can also overcome the conventional diffraction-limit that limits the

Manuscript received Mar. 15, 2009; revised Sept. 20, 2009; accepted Oct. 5, 2009.

Wing-Ying Kwong (email: optoelectronic@ymail.com) is a freelance researcher in the field of optoelectronics, Spring Hill, FL, USA.
doi:10.4218/etrij.10.0109.0173

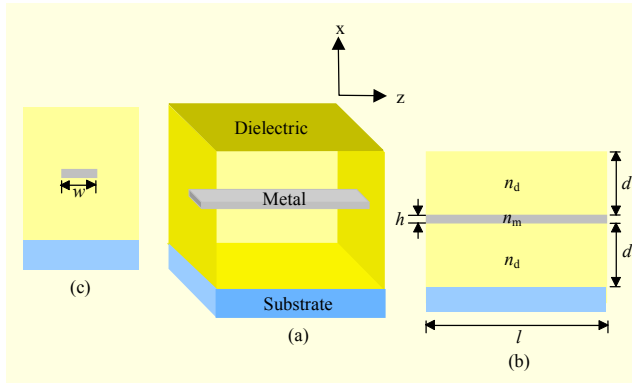


Fig. 1. (a) An SPP waveguide nano-structure: (b) front view and (c) side view with dimensions.

minimum size of conventional optical components and devices, allowing their dimensions to be further reduced to much smaller than the wavelength of light (that is, sub-wavelength sizes). Thus, the size of plasmonic waveguide devices is limited only by dimensions of the input/output coupler and the propagating or transmitting medium.

II. Principles of Plasmonic Waveguides and Their Functional Devices

SPP single-mode waveguides are sub-wavelength components in miniaturized opto-electronic circuits that may either be used to guide plasmonic signals to various parts of a circuit or to develop functional devices with functions achieved by active-controlling confined guided waves.

1. Waveguide-Device Physics

SPP single-mode waveguides may be constructed with a thin lossy metal film stripe of thickness h , length l , and finite width w embedded in a dielectric medium (see Fig. 1). The symmetrically divided upper and lower dielectric media have an equal thickness of d and the whole structure is placed on a substrate as in Fig. 1(b).

An SPP mode may be excited by the end-coupling (pig-tailing) method, where a lightwave is fed onto the polished or cleaved metallic waveguide end-face that has a rough surface, with the input lightwave profile closely matching that of the guided wave to be excited. This incident light, having a frequency of ω , then interacts with mobile surface electron-charges that have a frequency of ω_p to give rise to the electromagnetic SPP mode with an enhanced field strength that is confined to the nano-scale dimension of the metal surface. The confined SPP mode, with $\omega < \omega_p$, is thus tightly bound to the planar metal surface. It is guided by this surface and propagates with its energy dissipating as heat as a result of

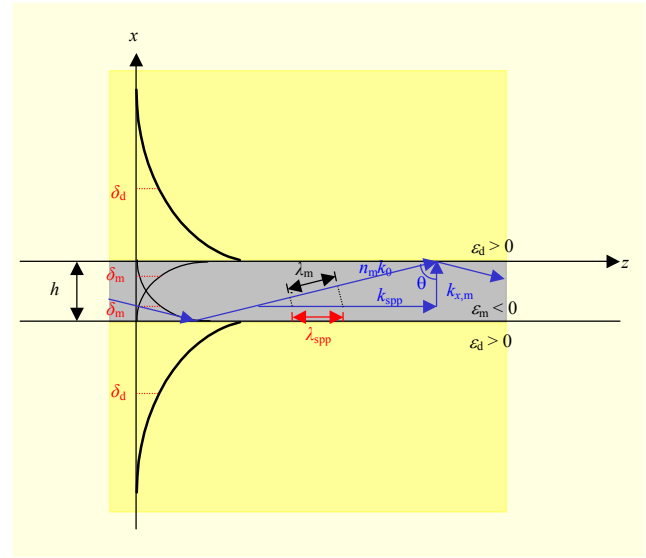


Fig. 2. Two TM SPP waves at dielectric-metal and metal-dielectric interfaces are coupled in the metal film stripe and propagate in the z -direction; while field amplitudes H_y , or E_z , tail-off in the x -direction. Penetration depths of the SPP wave into the dielectric and into the metal and the wavelength of the symmetric SPP mode are shown in red. Also shown is the SPP wave-vector diagram in blue.

electron-lattice-imperfection collisions in the metal; these ohmic losses consequently limit the propagation distance, z , of SPP modes. On the other hand, the mode-field must vanish at infinity (that is, no energy should flow) in the transverse direction. This necessary condition requires the mode-field to decay exponentially in the surrounding upper and lower dielectric media, away from the surface, in the x -direction normal to metal-dielectric interfaces (see Fig. 2). Thus, the dielectric media must be sufficiently thick to include all the fields inside. On the other hand, the metal film stripe must be sufficiently thin so that the two SPP electric mode-fields associated with the upper and the lower interfaces overlap and couple with each other efficiently to form two fundamental SPP stripe-modes, of which the lower-energy tangential, or symmetric, mode (upper and lower SPP mode-fields in-phase with one another) is considered here for applications purposes. The thin metal film thickness should be on the order of 50 nm for most metals at optical frequencies to support the single stripe-SPP-mode propagation. By varying the thickness of the metal film stripe, the frequency and the wavelength λ of this stripe-mode may also be varied.

The use of a dielectric gain medium can compensate for metal losses, allowing SPP modes to propagate along the metallic nanostructure without loss. In view of functional waveguide devices, the metal-dielectric hybrid waveguide structure is used, where the dielectric is treated as another

waveguide. Energy can be transferred from the dielectric gain medium to the propagating SPP mode, localizing it in the metal surface. The thin metal film stripe confines the lasing mode to the dielectric gain medium, with the SPP mode guiding the lasing mode. Thus, propagating modes in the gain dielectric can be controlled by SPP modes, or vice versa.

2. Properties of Metals

Metals play a major role in plasmonic waveguides and their devices. The conductivities of metals can be generally explained by the classical Drude model, from which the theory of optical properties of metals may be deduced. This model treats free electrons in metals as oscillators and solves the equation of motion under an applied electric field, \mathbf{E} , to give the displacement of an electron from its initial position or from an ion. This displacement subsequently gives rise to an electric dipole moment. For a volume of electrons, the volume density of electric dipole moments is obtained and the expression for this induced electric polarization, \mathbf{P} , in the metal may be written as

$$\mathbf{P}(\omega) = \varepsilon_0 \chi_e(\omega) \mathbf{E}(\omega), \quad (1)$$

where χ_e is the electric susceptibility. Applying (1) to the electric displacement relation, \mathbf{D} , one obtains

$$\mathbf{D}(\omega) = \varepsilon_0 \mathbf{E}(\omega) + \mathbf{P}(\omega) = \varepsilon_0 \varepsilon_m(\omega) \mathbf{E}(\omega), \quad (2)$$

where $\varepsilon_m(\omega) = 1 + \chi_e(\omega)$ is the dielectric function or relative permittivity of the metal. The equivalent permittivity of the electron-plasma, $\varepsilon_p(\omega)$, may then be defined as

$$\varepsilon_p(\omega) = \varepsilon_0 \varepsilon_m(\omega), \quad (3)$$

from which the intrinsic impedance of the plasma, $\eta_p(\omega)$, is obtained:

$$\eta_p(\omega) = \frac{\eta_0}{\sqrt{\varepsilon_m(\omega)}}, \quad (4)$$

where η_0 is the free-space intrinsic impedance.

The Drude model assumes that the metal is a good or an ideal conductor. Predictions from this model agree well with reported experimental data for most metals operated at wavelengths of 1 μm and longer, which covers nearly the whole infrared spectrum.

Optical properties of metals are characterized by the complex refractive index n_m of an absorbing medium:

$$n_m = n'_m - j\kappa, \quad (5)$$

where n'_m is the index of refraction, and κ is the extinction coefficient that is responsible for the evanescence of an optical wave. Both optical constants, n'_m and κ , are wavelength- and

temperature-dependent. At optical frequencies, ε_p is a complex number and is related to n_m by $\varepsilon_p n_m^2$. Matching this relation with that in (3), we obtain

$$\varepsilon_m = n_m^2, \quad (6)$$

$$\varepsilon'_m - j\varepsilon''_m = (n'_m - j\kappa)^2 = (n_m'^2 - \kappa^2) - j2n'_m\kappa, \quad (7)$$

where ε'_m is a real constant and ε''_m is responsible for the absorption and scattering losses in the metal. Matching dielectric constants with optical constants in (7), one obtains

$$\varepsilon'_m = n_m'^2 - \kappa^2 \quad \text{and} \quad (8a)$$

$$\varepsilon''_m = 2n'_m\kappa, \quad (8b)$$

where optical constants are determined by reflection methods. From (7), we can also solve for optical constants in terms of dielectric constants, yielding

$$n_m'^2 = \frac{1}{2} [\sqrt{\varepsilon_m'^2 + \varepsilon_m''^2} + \varepsilon'_m] \quad \text{and} \quad (9a)$$

$$\kappa^2 = \frac{1}{2} [\sqrt{\varepsilon_m'^2 + \varepsilon_m''^2} - \varepsilon'_m], \quad (9b)$$

where dielectric constants may be determined through the use of the mean time between electron collisions with lattice thermal vibrations or by the attenuated total reflection minimum method [1].

With these optical and dielectric constants, it is useful to define figures-of-merit (FOMs) for metal-materials to be used in plasmonic devices as parameters for the measurement of device performance or selection of metals for plasmonic waveguide structures. A reflectivity FOM, M_R , which depends on optical properties of metals, measures reflectivity efficiencies of metal materials and is expressed as

$$M_R = \frac{n'_m}{\kappa}. \quad (10)$$

For $n'_m \ll \kappa$ ($M_R \approx 0$), reflectivities of light from metal surfaces are nearly 100%, particularly at the end-coupling excitation type of incidence. For an ideal metal, $n'_m = 0$ ($M_R = 0$), $n_m^2 = -\kappa^2 < 0$ and $\varepsilon_m = \varepsilon'_m < 0$. The propagating lightwave is always evanescent and the reflectivity of light from such a metal surface is always 100%. Such metal provides the total internal reflection for well-confined mode propagation. Thus, the smaller the M_R value, the higher the reflectivity. Another useful FOM is the loss FOM, M_{L1} , which depends on the material properties of metals. It measures the losses of metal materials and is expressed as

$$M_{L1} = \frac{\varepsilon''_m}{\varepsilon_m'^2}. \quad (11)$$

The smaller the M_{L1} , the lower the resistive heat loss or

Table 1. Properties of selected polycrystalline metals at $\lambda=3.10 \mu\text{m}$ at room temperature.

Metal	n_m	M_R	ϵ_m	M_{L1} ($\times 10^{-4}$)	M_{L2} ($\times 10^{-4}$)
Beryllium	$2.07-j12.6$	0.1643	$-154.48-j52.16$	21.86	19.62
Copper	$1.59-j16.5$	0.0964	$-269.72-j52.47$	7.21	6.95
Gold	$1.73-j19.2$	0.0901	$-365.65-j66.43$	4.97	4.81
Tungsten	$1.94-j13.2$	0.1470	$-170.48-j51.22$	17.62	16.16

ohmic loss in the metal. A third FOM, M_{L2} , which is a variation of M_{L1} , is useful in measuring metal losses under the presence of gain and is expressed as

$$M_{L2} = \frac{\epsilon_m''}{|\epsilon_m|^2}. \quad (12)$$

One of the physical properties of interest for metals is the crystal structure, which is important when stability is a concern. Crystals with cubic and hexagonal structures exhibit structure-type dependent anisotropies that do not appear in the polycrystalline structure. Polycrystalline metals are of random texture that may be induced by growth and processing conditions. Nearly all common metals are polycrystalline.

For wavelengths between $2 \mu\text{m}$ to $5 \mu\text{m}$, $n_m' \ll \kappa$ or ϵ_m has a large negative ϵ_m' and a small positive ϵ_m'' at room temperature, so that we may make the general assumption that $|\epsilon_m'| \gg |\epsilon_m''|$. Table 1 lists refractive indices [2] and calculated relative permittivities and figures of merit of selected polycrystalline metals at $\lambda=3.10 \mu\text{m}$ at room temperature. Among the metals listed in the table, gold exhibits the highest reflectivity efficiency and the lowest heat loss.

3. SPP Propagation

Propagation characteristics of SPP modes may be derived using the structure shown in Fig. 3. In this model, the SPP wave propagates along the planar interface between two semi-infinite media, namely, a dielectric having a positive dielectric constant of n_d^2 and a continuous planar metal having a negative dielectric constant of n_m^2 . This is just the upper-half of the model shown in Fig. 2 if we consider the upper interface.

When an incident light hits the polished or cleaved metallic waveguide end-face, the lightwave is scattered in all directions, while the transmitted wave propagates at an angle, θ , to the normal of the interface and undergoes total internal reflections at the interface (see Fig. 2). This SPP wave has a propagation constant $n_m k_0$ (where $k_0 = \omega/c$ is the free-space wave-number of a lightwave) in the wave-normal direction, which may be decomposed into two components, k_z and $k_{x,m}$. At resonance,

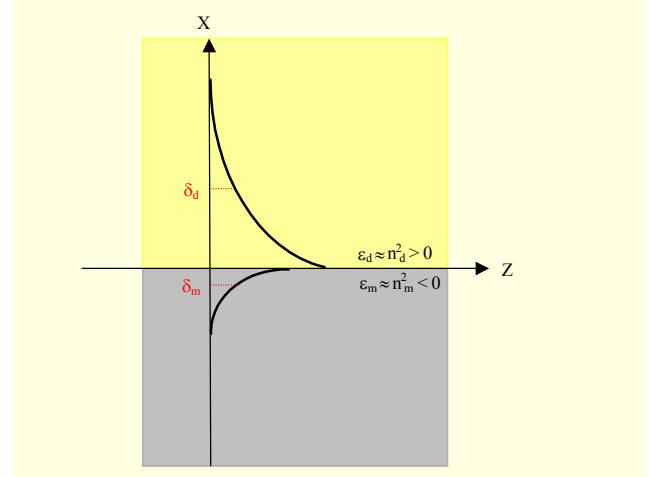


Fig. 3. An SPP mode at a planar interface between two semi-infinite media, a dielectric having a positive dielectric constant of n_d^2 and a continuous planar metal having a negative dielectric constant of n_m^2 .

$k_z = k_{spp}$ so that $k_{spp} = k_0 n_m \sin \theta$ is the wave-vector component of the SPP mode that is parallel to the interface, and $k_{x,m} = k_0 n_m \cos \theta$ is the wave-vector component that is normal to the interface. This right triangle arrangement of wave-vectors allows us to apply the Pythagorean theorem to write $k_{spp}^2 + k_{x,m}^2 = n_m^2 k_0^2$. This analytical relation, which is based on ray optics, may also be obtained from the wave equation for the SPP mode function, which holds separately in each medium of the structure shown in Fig. 3; thus, the derived relation [1], [3] becomes

$$k_{spp}^2 + k_{x,i}^2 = \epsilon_i k_0^2 \quad \text{or} \quad (13a)$$

$$k_{x,i} = \sqrt{\epsilon_i k_0^2 - k_{spp}^2}, \quad i = d, m, \quad (13b)$$

where $\epsilon_i = n_i^2$ and $k_{x,i}$ is termed as the mode-field attenuation constant in the x -direction.

The mode condition that determines the propagation characteristics of TM SPP modes can be obtained by solving the SPP wave equation subject to the continuity condition on tangential field components at the interface. This mode condition may then be solved to yield the axial propagation constant [3] β , where

$$\beta = k_0 \sqrt{\frac{n_m^2 n_d^2}{n_m^2 + n_d^2}}. \quad (14)$$

To evaluate dispersion characteristics of SPP modes, we rewrite (14) in terms of their respective relative permittivities to yield the dispersion relation for the SPP propagation:

$$k_{spp} = \frac{\omega}{c} \sqrt{\frac{\epsilon_m \epsilon_d}{\epsilon_m + \epsilon_d}}, \quad (15)$$

where k_{spp} is termed as the propagation constant in the

z -direction. Confined SPP mode propagation requires that k_{spp} is real. The dielectric medium should not be significantly dispersive, so that $|\epsilon_m| \gg |\epsilon_d|$, and k_{spp} is always larger than $\omega/c = k_0$, which implies that the momentum ($\hbar k$) of SPP modes is always greater than that of light in free space. Since $k_{\text{spp}} > k_0$, by inspection of (13), $k_{x,i}$ must be imaginary. The real k_{spp} and the imaginary $k_{x,i}$ thus explain the characteristic of an SPP mode at an interface—the mode-fields are at their maximum at the interface and decay exponentially away from that interface.

A. Waveguide Parameters under the Absence of Gain

For the spectral region of interest, n_m^2 and thus ϵ_m become complex. While the fundamental SPP mode propagates along the dielectric-metal interface, the mode-power attenuation due to ohmic losses causes β to become complex:

$$\beta = \beta' - j \frac{\alpha}{2}, \quad (16)$$

where β' is the phase constant, and α is the power attenuation coefficient. The complex ϵ_m implies that k_{spp} is also complex, so that (15) becomes

$$k_{\text{spp}} = k'_{\text{spp}} - j k''_{\text{spp}} \approx k_0 \sqrt{\frac{\epsilon_d \epsilon'_m}{\epsilon_d + \epsilon'_m}} \left[1 - j \frac{\epsilon''_m \epsilon_d}{2 \epsilon'_m (\epsilon_d + \epsilon'_m)} \right]. \quad (17)$$

Matching the real and the imaginary parts of this equation with those of (16) and making use of (11), we obtain

$$k'_{\text{spp}} \equiv \beta' = k_0 \sqrt{\frac{\epsilon_d \epsilon'_m}{\epsilon_d + \epsilon'_m}} \quad (18a)$$

and

$$k''_{\text{spp}} \equiv \frac{\alpha}{2} \approx \frac{k_0}{2} \frac{\epsilon''_m \epsilon_d^{3/2}}{\sqrt{\epsilon'_m (\epsilon_d + \epsilon'_m)^3}} = \frac{k_0}{2} (M_{\text{L1}}) \left(\frac{\epsilon'_m \epsilon_d}{\epsilon'_m + \epsilon_d} \right)^{3/2}, \quad (18b)$$

respectively. Here, k_{spp}' denotes the wavelength of the SPP mode, and λ_{spp} (see Fig. 2) and k_{spp}'' denote the propagation length of the SPP mode, δ_{spp} . Applying the relation $k = 2\pi/\lambda$ to (18a), we obtain

$$\lambda_{\text{spp}} = \frac{2\pi}{k'_{\text{spp}}} = \lambda_0 \sqrt{\frac{\epsilon'_m + \epsilon_d}{\epsilon'_m \epsilon_d}}, \quad (19)$$

where λ_0 is the free-space wavelength. For $|\epsilon'_m| \gg |\epsilon_d|$, λ_{spp} is always less than λ_0 , which suggests possible applications in shorter-wavelength electromagnetic wave-guiding. The SPP propagation length may be found by using the relation $\delta = 1/\alpha$ with (18b), yielding

$$\delta_{\text{spp}} = \frac{1}{2k''_{\text{spp}}} = \frac{\lambda_0}{2\pi} (M_{\text{L1}})^{-1} \left(\frac{\epsilon'_m + \epsilon_d}{\epsilon'_m \epsilon_d} \right)^{3/2}. \quad (20)$$

Comparing this equation with (19), we can see that $\delta_{\text{spp}} \gg \lambda_{\text{spp}}$, which means that we may use periodic surface structures (such as gratings) to manipulate SPPs, which allows these modes to interact with such structures over several periods.

In a plasmonic circuit, an optical signal often fades away quickly during transmission in the SPP waveguide before reaching the destination because of the short propagation length. To increase the propagation length, we may choose a low-loss metal or a metal of high reflectivity efficiency, such as copper, gold (Table 1) or silver. Another option is to decrease the metal film thickness in order to decrease the attenuation of the SPP mode, but with the mode-field extended further into the dielectric.

Penetration depths, or attenuation lengths, of the SPP mode-field into the dielectric δ_d and into the metal δ_m (Figs. 2 and 3) may be found by taking the inverse of the magnitudes of their respective attenuation constants, that is, $\delta_i = 1/|k_{x,i}|$ and $i = d, m$. Thus, after applying (15) to (13b) and substituting, we obtain

$$\delta_d = \frac{1}{|k_{x,d}|} = \frac{1}{k_0} \sqrt{\frac{\epsilon'_m + \epsilon_d}{\epsilon_d^2}} \quad (21a)$$

and

$$\delta_m = \frac{1}{|k_{x,m}|} = \frac{1}{k_0} \sqrt{\frac{\epsilon'_m + \epsilon_d}{\epsilon_m^2}}, \quad (21b)$$

respectively. For $k_0 = 2\pi/\lambda_0$ and $|\epsilon_m| \gg |\epsilon_d|$, $\delta_d(\lambda_0)$ is proportional to $|\sqrt{\epsilon_m}|$, which indicates that the field penetrates deeper into the dielectric as $|\epsilon_m|$ increases; while $\delta_m(\lambda_0)$ is inversely proportional to $|\sqrt{\epsilon_m}|$, which indicates that sizes of plasmonic waveguides miniaturize as $|\epsilon_m|$ increases. Here, δ_d measures the sensitivity of the SPP mode to refractive-index changes, while δ_m indicates the minimum metal film thickness to be used.

B. Propagation in the Presence of Gain

To compensate for ohmic losses in the metal, gain—a complicated function of doping levels, current density, temperature, and frequency—is introduced into the dielectric medium to improve the propagation length or to achieve lossless propagation. This causes the relative permittivity of the dielectric to become complex; that is, $\epsilon_d = \epsilon'_d + j\epsilon''_d$. The dispersion relation in (15) can thus be written as

$$k_{\text{spp}}^2 = k_0^2 \frac{(\epsilon'_m - j\epsilon''_m)(\epsilon'_d + j\epsilon''_d)}{(\epsilon'_m + \epsilon'_d) - j(\epsilon''_m - \epsilon''_d)}. \quad (22)$$

Because ϵ''_m is negative and $|\epsilon'_m| \gg |\epsilon_d|$, one may also assume

Table 2. Propagation characteristics of SPP modes and required gain coefficients for lossless propagation.

λ_0 (μm)	Metal	Dielectric	n_m	ε_m	$M_{12} (\times 10^{-4})$	$\varepsilon'_d, \varepsilon'_d$	λ_{spp} (nm)	δ_{spp} (μm)	δ_m (nm)	δ_d (nm)	$ g $ (cm^{-1})
2	Ag	AlAs	0.65-j12.2	-148.42-j15.86	7.12	8.24	677.25	17.17	26.76	484.98	529.08
2	Cu	AlAs	0.85-j10.6	-111.64-j18.02	14.09	8.24	670.66	8.30	31	425.65	1047.01
5	Fe	GaAs	4.59-j15.4	-216.09-j141.37	21.20	10.88	1477.42	6.78	50.55	1200.19	956.07
5	Fe	InP	4.59-j15.4	-216.09-j141.37	21.20	9.49	1587.34	8.41	50.42	1372.54	778.83

that $|\varepsilon_m| \gg |\varepsilon'_d|, |\varepsilon''_d|$. Assuming that a metal of high reflectivity efficiency is used, by separating (22) into real and imaginary parts and making use of (12), we obtain

$$k_{\text{spp}}^2 \approx \frac{k_0^2}{(\varepsilon'_m + \varepsilon'_d)^2} \times \left\{ \left(\varepsilon'_d |\varepsilon_m|^2 + \varepsilon'_m |\varepsilon_d|^2 \right) + j(-\varepsilon''_m) \left[\varepsilon_d'^2 - (M_{12})^{-1} \varepsilon_d'' + \varepsilon_d'^2 \right] \right\}, \quad (23)$$

where $|\varepsilon_i|^2 = (\varepsilon'_i)^2 + (\varepsilon''_i)^2$, $i = d, m$. To find the amount of gain that fully compensates metal losses for lossless propagation, we set the imaginary part of (23) to zero and solve for ε_d'' , yielding

$$\varepsilon_d'' \approx (M_{12})(\varepsilon_d')^2; \quad (24)$$

thus, the complex ε_d becomes $\varepsilon_d' + j[(M_{12})(\varepsilon_d'^2)]$. We can see that lower loss indicates that less gain is required for lossless propagation.

The power gain coefficient g may then be obtained by interchanging the subscripts d and m in (18b), followed by linearly transforming α via a sign change ($g = -\alpha$). Under the condition that $|\varepsilon_m| \gg |\varepsilon'_d|$, we obtain

$$g = -k_0 \frac{\varepsilon_d''}{\sqrt{\varepsilon'_d}}.$$

By substituting (24) for ε_d'' for lossless propagation and using the definition of k_0 , we obtain the required gain coefficient to compensate for metal losses as

$$g = -\frac{2\pi}{\lambda_0} (M_{12})(\varepsilon_d')^{3/2}. \quad (25)$$

Thus, as gain is added from initial $g_0=0$ into the dielectric, the propagation length begins to increase until the gain reaches $|g|$, then lossless SPP propagation is achieved. This method of controlling the SPP propagation serves as a basis for modulators and switches, which are typical examples of plasmonic functional devices integrated into plasmonic optoelectronic circuits, or plasmonic chips.

Table 2 summarizes the propagation characteristics of SPP modes in four different plasmonic waveguides of sub-wavelength sizes (δ_m). With $\delta_d \approx \lambda_0/4$, the sizes of these whole waveguide structures turn out to be approximately $\lambda_0/2$. Table 2

also lists the gain coefficients necessary to compensate for metal losses. As gain represents a loss in the dielectric, gain requirements should be as low as possible. As seen in (25), the wavelength band of interest clearly has a lower gain requirement than shorter wavelengths in the mid-infrared band, such as the telecommunication wavelength of 1.55 μm , because of the λ_0^{-1} dependence. When all parameters in (25) vary, the gain requirement may or may not be lowered. For example, if we increase λ_0 from 2 μm to 5 μm and increase ε'_d to larger than 8.24, then, $|g|$ will be lowered if a slightly more lossy metal is used. However, $|g|$ will be increased if a very lossy metal is used. When λ_0 and ε'_d are kept constant, $|g|$ is proportional to M_{12} . That is, lower-loss metals can reduce gain requirements. When λ_0 and M_{12} are kept constant, as ε'_d decreases, $|g|$ decreases, which suggests that a lower refractive index for the dielectric may be used to reduce the gain requirement.

III. Optimization of Device Performance

In practice, besides absorption losses in metals, we should take into account additional losses, such as scattering losses (due to surface roughness and metal-stripe edges) and grain boundaries, which can increase the gain requirement. Advanced deposition techniques, such as nano-fabrication, and good surface quality may improve the gain requirement and should be carefully considered when preparing samples. Besides introducing gain into the dielectric medium to compensate for ohmic losses in metals, the volume of the metal itself can be reduced to its smallest possible dimension in order to reduce ohmic losses. The high reflection from metals can be compensated by matching impedances on metals. Both absorption and scattering in the dielectric also contribute to propagation losses.

For functional devices, the insertion loss associated with metal electrodes should also be reduced. By using a buffer layer with a lower refractive index (for example, a layer that has a different weight in chemical composition than the metal) to relax the metal's effect on guided modes and for better confinement in the dielectric, propagation loss due to the metal-dielectric interface can be reduced to an insignificant level by

increasing the buffer-layer thickness.

The symmetrical SPP waveguide structure offers the lowest SPP propagation loss among SPP waveguide structures of proper dimensions. For a functional SPP-waveguide device, where another guided wave, excited by an external optical excitation or a temperature change in the dielectric medium, interacts with the SPP mode, the waveguide structure becomes asymmetrical as a consequence of the refractive index change. Since the SPP propagation loss depends on the refractive-index difference between top and bottom dielectric layers, the greater the asymmetry, the higher the propagation loss and the shorter the propagation length. This asymmetry causes the SPP mode depth profile (depth mode-field diameter, DMFD) to change from a symmetric profile to an asymmetric profile as well. The DMFD, depending on the thickness of the metal stripe, determines the tightness of the SPP mode that is bound to the metal surface and can be tuned by the thickness of the dielectric. Reducing the dielectric thickness increases the propagation loss as does reducing the metal film thickness. However, this also allows the mode to become better confined. Thus, there is a trade-off between mode size and propagation loss.

A metal film stripe with a finite width w , as in Fig. 1(c), is treated as a core surrounded by a dielectric. Generally, the propagation loss decreases as w decreases, indicating a very low propagation loss may be achieved by reducing w . However, when w becomes narrower than a certain width, no guided modes can exist in the metal stripe. This causes propagation lengths to become zero, which limits the propagation on the stripe. Nevertheless, for micro-meter-wide stripes, the lateral MFD (LMFD), depending on the width of the metal stripe, determines the confinement of the SPP mode. Reducing w causes the LMFD to decrease at first, but at a certain w , LMFD starts to increase, showing a poor light confinement with too-narrow metal stripes. Consequently, the DMFD increases. For the asymmetrical SPP waveguide structure, decreasing w also decreases the propagation length; thus, there is a trade-off between confinement and propagation length. From these features of SPP-mode depth and lateral profiles, we conclude that coupling losses at one end of the metal stripe waveguide will increase as w decreases. Therefore, by choosing a proper metal film stripe dimension, we can reduce the coupling loss, with SPP mode profiles matching closely with those of the incident mode.

For highly efficient functional waveguide devices, careful selection of practical materials allows the minimization of losses, such as propagation loss and transmission loss, and facilitates fabrication processes. An optimally low propagation loss requires an optically transparent material with minimal surface roughness and guided-wave scattering. This material

should also be highly purified after fabrication processes in order to avoid unnecessary absorption by impurities. The availability of new semiconductor laser materials that can operate in the longer 2 μm to 5 μm mid-infrared wavelength band allows plasmonic waveguide devices to be constructed with a minimal loss value much lower than that found in the shorter mid-infrared wavelength band. This extremely low-loss dielectric gain material system includes fluorides, chalcogenides, halides and III-V compound semiconductor nano-crystals. At optical frequencies, the choice of a metal material for the plasmonic waveguide structure becomes crucial. Highly confined mode propagation requires a metal to have high reflectivity efficiency so as to lower the operating power and thus reduce the heat loss in the metal. Among polycrystalline metals, the three candidate metals for lowest losses are silver, gold, and copper, in that order. Recently, an artificial negative-index material, metamaterial, was found to have the capability of mimicking the response of a metal to electromagnetic waves when $\omega < \omega_p$, that is, the negative ϵ_m . Metamaterials have fascinating unprecedented pre-designed electromagnetic properties and functionalities that promise to open up a new prospect in manipulating light, revolutionizing today's optical technologies for better electronic system performance.

IV. Conclusion

For highly efficient data communication, the most important factor is to minimize propagation losses and transmission losses. At wavelengths in the 2 μm to 5 μm mid-infrared region, compensated plasmonic waveguides, with a structure of a nanometer-thin polycrystalline metal embedded in a dielectric gain medium and a reduced whole-structure size of approximately half of the operating free-space wavelength, offer the possibility to transmit plasmonic signals with negligible (or without) losses. Functional plasmonic waveguide devices of the metal-dielectric hybrid waveguide structure may then be implemented by active guided-wave control of these plasmonic signals. By optimizing the plasmonic waveguide geometry and carefully selecting low-loss waveguide materials, we can further reduce the gain requirement and other losses, enabling SPP-based functional waveguide devices to operate more efficiently. With the proper choice of processing conditions in nano-imprinting, low-cost, high-fidelity, and highly-ordered arrays of sub-wavelength nano-structured photonic components can be rapidly mass-produced.

References

- [1] H. Raether, *Surface Plasmons on Smooth and Rough Surfaces and on Gratings*, Berlin: Springer-Verlag, 1988.

- [2] M. Bass, editor-in-chief, *Handbook of Optics*, 2nd ed., New York: McGraw-Hill, Inc., 1995.
- [3] A. Yariv and P. Yeh, *Optical Waves in Crystals*, New York: John Wiley and Sons, Inc., 1984.



Wing-Ying Kwong received the BS degree in computer science from the State University of New York at Stony Brook, New York, USA, in 1981. She was a software engineer with Hazeltine Corporation from 1981 to 1986 and pursued graduate studies in electrical engineering at the State University of New York

at Stony Brook from 1982 to 1988. She received the MSE degree in electrical engineering from the City College of the City University of New York, New York, USA, in 1994. From 1998 to 1999, she was a PhD researcher in optics with the Department of Electrical Engineering of the City University of New York, working on experimental single organic-layer light emitting diodes. Since 1999, she has been a freelance researcher in optoelectronics. She is a senior member of the IEEE and a member of the SPIE professional societies. Her current research interests include integrated optics, optical/photonic integrated circuits, nanophotonics, lightwave propagation, and light-matter interaction.